

# On the presence of high nitrite ( $\text{NO}_2^-$ ) in coarse particles at Mt. Qomolangma

Zhongyi Zhang<sup>1, 2</sup>, Chunxiang Ye<sup>3</sup>, Yichao Wu<sup>1</sup>, Tao Zhou<sup>4</sup>, Pengfei Chen<sup>5, 6</sup>, Shichang Kang<sup>5, 6</sup>, Chong Zhang<sup>3</sup>, Zhuang Jiang<sup>1</sup>, Lei Geng<sup>1, 2, 4\*</sup>

<sup>1</sup>Deep Space Exploration Laboratory/School of Earth and Space Sciences, University of Science and Technology of China, Hefei 230026, Anhui, China

<sup>2</sup>CAS Center for Excellence in Comparative Planetology, University of Science and Technology of China, Hefei 230026, Anhui, China

<sup>3</sup>SKL-ESPC & SEPKL-AERM, College of Environmental Sciences and Engineering, and Center for Environment and Science, Peking University, Beijing 100871, China

<sup>4</sup>National Key Laboratory of Deep Space Exploration, Hefei, 230088, Anhui, China.

<sup>5</sup>Key Laboratory of Cryospheric Science and Frozen Soil Engineering, Northwest Institute of Eco-Environment and Resources, Chinese Academy of Sciences; Lanzhou, 730000, Gansu, China

<sup>6</sup>University of Chinese Academy of Sciences; Beijing, 100049, China

\*Corresponding author: Lei Geng (Email: [genglei@ustc.edu.cn](mailto:genglei@ustc.edu.cn); Tel: +86-0551-63600015)

Summary: 8 pages, 2 texts, 1 table, and 3 figures.

Contents of this file

Text S1 Isotopic analysis of TSP and soil nitrate;

Text S2 Simulation of liquid water content and pH of TSP;

Figure S1. The heatmap showing the correlations among TSP water-soluble inorganic ions;

Figure S2. The relationships between TSP nitrite concentration with isotopic compositions;

Figure S3. The modelled TSP acidity and liquid water contents;

Table S1 The nitrate isotopic signatures in TSP.

## Text S1 Stable isotope compositions in TSP and soil nitrate

After the analysis of isotopic compositions in TSP  $\text{NO}_2^-$ , the remaining extracts of TSP samples were subsequently used for nitrate isotopic analyses via the bacterial denitrifier method<sup>1,2</sup>. Note that the nitrate isotopic composition was determined for a few TSP samples, as the extracts had been used for nitrite isotopic analysis and the available TSP amount were limited (i.e., 12h in flow rate of 30L/min). Before preparing the bacterial denitrifier method, nitrite in the TSP extracts were removed using sulfamic acid solution (0.3 mL, 1 mol L<sup>-1</sup>), followed by neutralization with high-purity sodium hydroxide solution. The nitrate in extracts were also converted into  $\text{N}_2\text{O}$  with the bacterial denitrifier method and then determined following the same procedures as described above. The international nitrate isotopic reference materials (USGS32, USGS34, and USGS35) were treated along with the samples for data calibrations. The standard deviations for  $\delta^{15}\text{N}$ ,  $\delta^{18}\text{O}$ ,  $\Delta^{17}\text{O}$  of  $\text{NO}_3^-$  reference materials were determined to be less than 0.2‰, 0.8‰, and 0.3‰, respectively. The nitrate isotopic signatures in TSP were presented in Table S1. The pre-concentrated soil extracts were also determined for nitrate isotopic compositions, and the soil nitrate isotopic compositions were presented in Table 1 in the main text.

## Text S2 Simulation of liquid water content and pH of TSP

Particulate nitrite (as pN(III)) undergoes thermodynamic exchange processes with HONO in the atmosphere. The potential thermodynamic partitioning between pN(III) and gaseous HONO (ratio of pN(III) to HONO) in Eq.1 is investigated based on aerosol pH and liquid water content<sup>3</sup>. The aerosol liquid water and acidity are predicted from the thermodynamic model ISORROPIA-II<sup>4</sup>. The performance of ISORROPIA-II in simulation the aerosol liquid water and acidity has been well-investigated in previous studies<sup>5,6</sup>.

$$\frac{[\text{pN(III)}]}{[\text{HONO}]} = H_{\text{HONO}} \left( 1 + \frac{k_1}{[\text{H}^+]} + \frac{[\text{H}^+]}{k_2} \right) \times R \times T \times \text{LWC} \quad (\text{Equation 1})$$

with  $H_{\text{HONO}}$  representing the gaseous HONO Henry's law partitioning coefficient (49M atm<sup>-1</sup>),  $k_1$  representing the acid dissociation constant ( $5.62 \times 10^{-4}$  M),  $k_2$  ( $\approx 0.02$  M) is the equilibrium constant of between the nitroacidium ion ( $\text{H}_2\text{ONO}_{(\text{aq})}^+$ ) and  $\text{HONO}_{(\text{aq})}$  in R2<sup>3</sup>. The  $[\text{H}^+]$  is the hydrogen ion concentration from the predicted particle pH using ISORROPIA-II. R is the gas constant, LWC is

the coarse particle liquid water content.

Observations of temperature, RH (>30%), the water-soluble inorganic ions were used as inputs to calculate aerosol pH and liquid water content. The nitrite is converted to an equimolar concentration of nitrate as the chemical system in ISORROPIA-II model does not incorporate nitrite chemistry. In this study, ISORROPIA-II is run in the “forward model”.

As expected, the modelled coarse particle LWC exhibits a significant contrast before and after April 30<sup>th</sup>, with mean values of 1.84  $\mu\text{g}/\text{m}^3$  and 0.89  $\mu\text{g}/\text{m}^3$ , respectively (Figure S3). The declines in LWC after April 30<sup>th</sup> can be attributed to decreased mass loadings of  $\text{NH}_4^+$ ,  $\text{SO}_4^{2-}$  and  $\text{NO}_3^-$  with high hygroscopicity. The TSP sample is characterized by a mildly basic pH (~7.5), which is reasonable because the majority of TSP (~3/4) in TP consists of mineral dust or lofted local soil <sup>7</sup>.

The ratio of  $[\text{pN(III)}]/[\text{HONO}]$  was estimated based on the modelled particle pH and LWC (Text S2, using ISORROPIA thermodynamic II model) and the Eq S1. The results indicated that the ratio of particulate  $\text{NO}_2^-$  to HONO concentration ( $[\text{pN(III)}]/[\text{HONO}]$ ) varied from 4.8 to 10.6 during the campaign. Note that the ratio of  $[\text{pN(III)}]/[\text{HONO}]$  maybe overestimated since the ISORROPIA II model does not incorporate the nitrite chemistry. While concurrent measurement of gaseous HONO was unavailable in this campaign, recent filed measurement found an average of ~30 pptv of gaseous HONO in the spring of 2019 in Namco site <sup>8</sup>, which is lower by ~5 times than our determined particulate  $\text{NO}_2^-$  concentration, analogues to the estimated  $[\text{pN(III)}]/[\text{HONO}]$  ratio.

## References

- (1) Sigman, D. M.; Casciotti, K. L.; Andreani, M.; Barford, C.; Galanter, M.; Böhlke, J. A bacterial method for the nitrogen isotopic analysis of nitrate in seawater and freshwater. *Anal. Chem.* **2001**, *73* (17), 4145-4153.
- (2) Casciotti, K. L.; Sigman, D. M.; Hastings, M. G.; Böhlke, J.; Hilkert, A. Measurement of the oxygen isotopic composition of nitrate in seawater and freshwater using the denitrifier method. *Anal. Chem.* **2002**, *74* (19), 4905-4912.
- (3) Chen, Q.; Edebeli, J.; McNamara, S. M.; Kulju, K. D.; May, N. W.; Bertman, S. B.; Thanekar, S.; Fuentes, J. D.; Pratt, K. A. HONO, Particulate Nitrite, and Snow Nitrite at a Midlatitude Urban Site during Wintertime. *ACS Earth Space Chem.* **2019**, *3* (5), 811-822. DOI: 10.1021/acsearthspacechem.9b00023.
- (4) Fountoukis, C.; Nenes, A. ISORROPIA II: a computationally efficient thermodynamic equilibrium model for  $\text{K}^+ - \text{Ca}^{2+} - \text{Mg}^{2+} - \text{NH}_4^+ - \text{Na}^+ - \text{SO}_4^{2-} - \text{NO}_3^- - \text{Cl}^- - \text{H}_2\text{O}$  aerosols. *Atmos. Chem. Phys.* **2007**, *7* (17),

4639-4659.

(5) Guo, H.; Liu, J.; Froyd, K. D.; Roberts, J. M.; Veres, P. R.; Hayes, P. L.; Jimenez, J. L.; Nenes, A.; Weber, R. J. Fine particle pH and gas–particle phase partitioning of inorganic species in Pasadena, California, during the 2010 CalNex campaign. *Atmos. Chem. Phys* **2017**, *17* (9), 5703-5719. DOI: 10.5194/acp-17-5703-2017.

(6) Weber, R. J.; Guo, H.; Russell, A. G.; Nenes, A. High aerosol acidity despite declining atmospheric sulfate concentrations over the past 15 years. *Nat. Geosci.* **2016**, *9* (4), 282-285. DOI: 10.1038/ngeo2665.

(7) Kang, S.; Chen, P.; Li, C.; Liu, B.; Cong, Z. Atmospheric aerosol elements over the inland Tibetan Plateau: Concentration, seasonality, and transport. *Aerosol Air Qual. Res.* **2016**, *16* (3), 789-800.

(8) Wang, J.; Zhang, Y.; Zhang, C.; Wang, Y.; Zhou, J.; Whalley, L. K.; Slater, E. J.; Dyson, J. E.; Xu, W.; Cheng, P.; et al. Validating HONO as an Intermediate Tracer of the External Cycling of Reactive Nitrogen in the Background Atmosphere. *Environ Sci Technol* **2023**, *57* (13), 5474-5484. DOI: 10.1021/acs.est.2c06731.

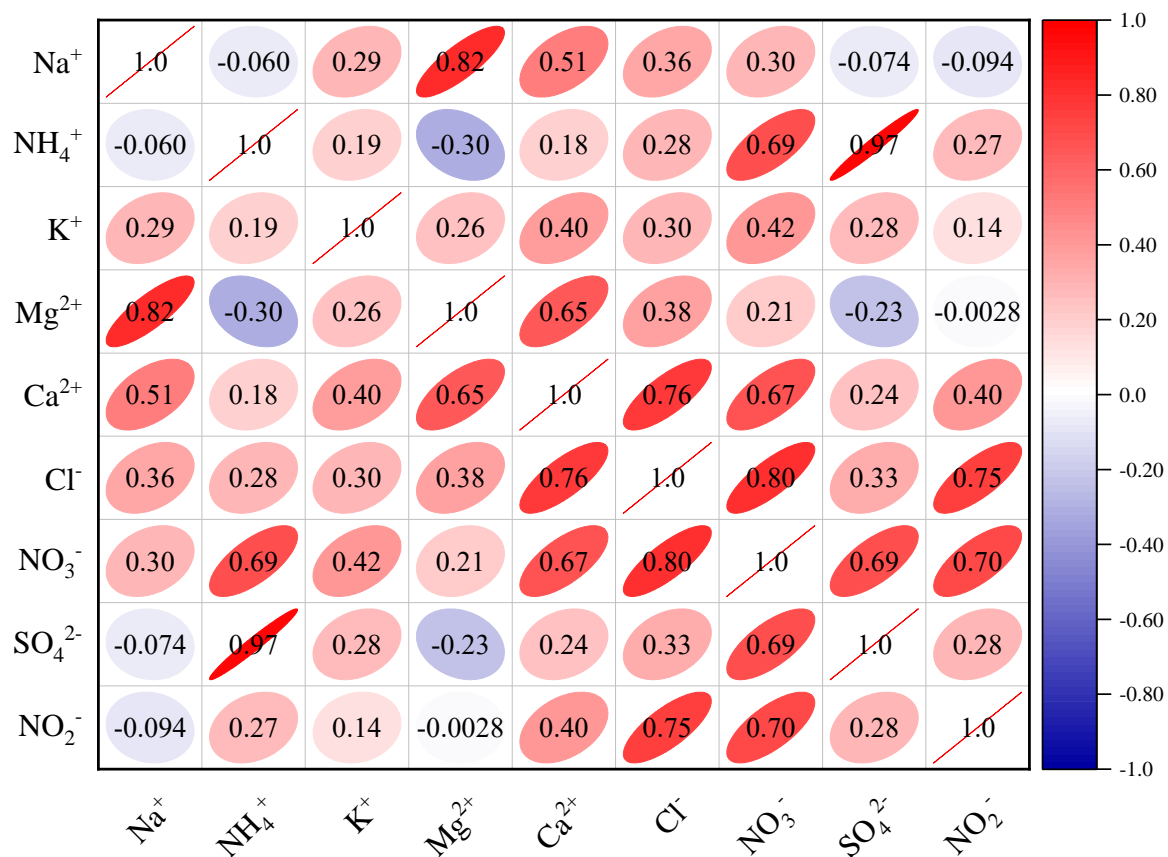
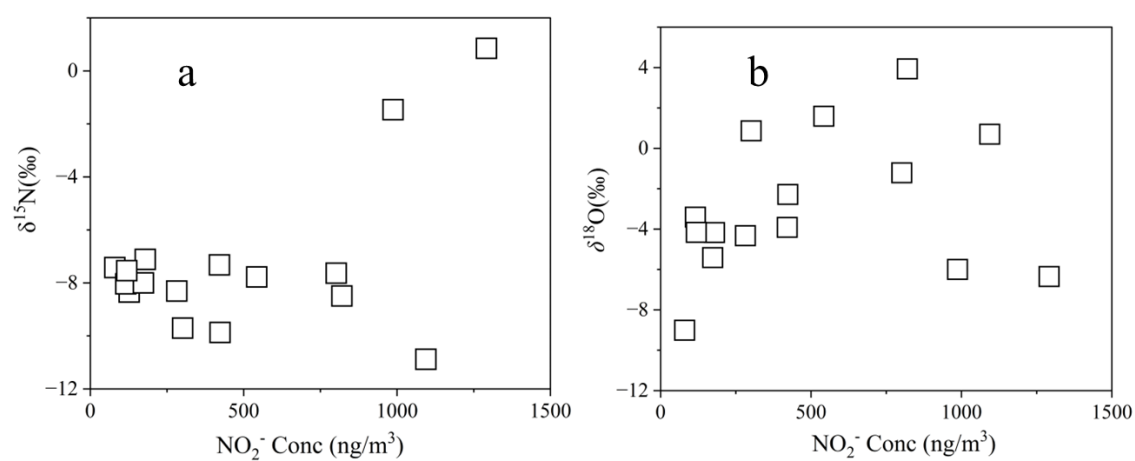


Figure S1 The correlation among the water-soluble inorganic ions in TSP samples collected samples collected at Base Camp, of Mt. Everest in spring 2022. The corresponded Pearson's r (correlation coefficient) is presented as overlapped heatmaps.



**Figure S2.** Relationship observed between the TSP nitrite concentration with  $\delta^{15}\text{N}$  (a) and  $\delta^{18}\text{O}$  (b) at Base Camp of Mt. Everest in spring 2022.

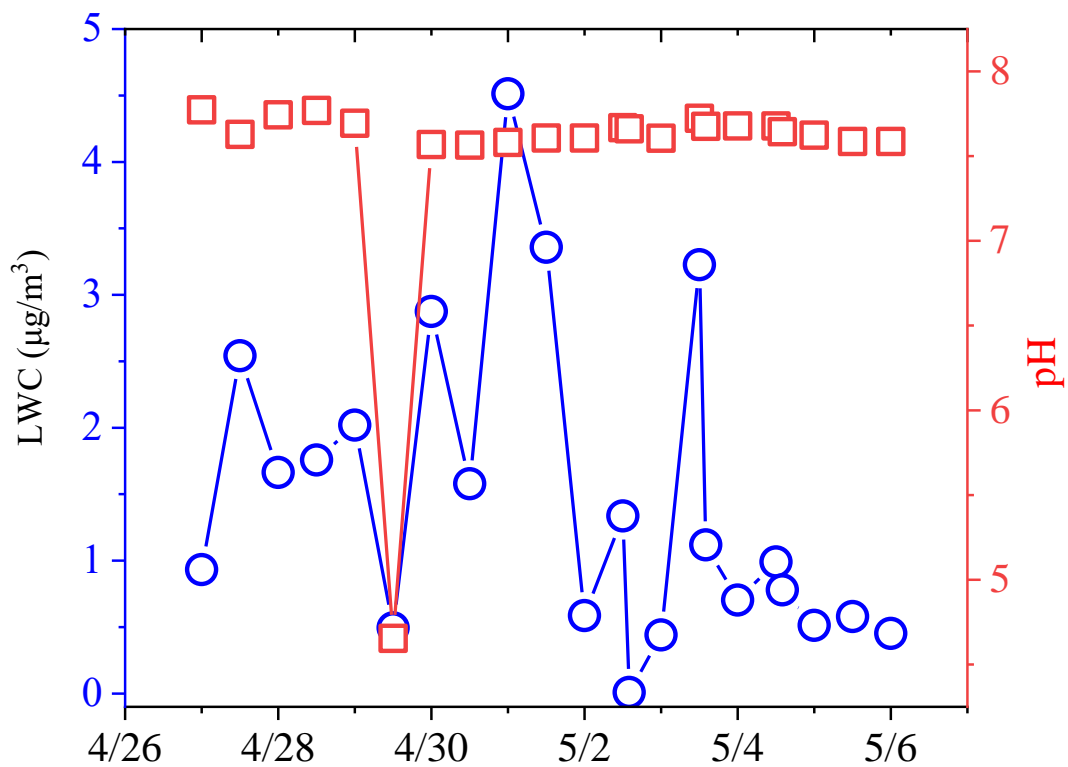


Figure S3. The predicted coarse particle liquid water content (LWC, blue circle) and acidity (red square) using the thermodynamic model ISORROPIA-II during “Earth Summit Mission” scientific expedition in spring 2022.,

Table S1 The nitrate isotopic signatures in TSP collected during the campaign of “Earth Summit Mission-2022” scientific expedition.

Sample ID	Sampling period	Conc (ng/m <sup>3</sup> )	$\delta^{15}\text{N}(\text{‰})$	$\Delta^{17}\text{O}(\text{‰})$
TSP-2	9:00-20:00, April 27	936	-5.2	22.1
TSP-4	9:00-20:00, April 28	1557	-8.8	18.2
TSP-5	21:00-8:00, April 27-28	1449	-0.7	29.5
TSP-6	9:00-20:00, April 29	1757	-6.3	24.0